Acousto-Optics—A Review of Fundamentals

ADRIANUS KORPEL, FELLOW, IEEE

Invited Paper

Abstract—**The paper first reviews the historical development of acousto-optics and its applications. Following this, a heuristic explanation of acousto-optic effects is presented, with the emphasis on the plane wave model of interaction. Finally, there is a discussion of some basic configurations of relevance to signal processing.**

I. Introduction

ACOUSTO-OPTICS deals with the interaction of sound and light. The existence of such an interaction was predicted by Brillouin [1] in 1922. Experimental verification followed in 1932, by Lucas and Biquard [2] in France, and Debye and Sears [3] in the U.S. Brillouin's original theory predicted a phenomenon closely analagous to X-ray diffraction in crystals. In the latter, the atomic planes cause multiple reflections of an incident electromagnetic plane wave. These reflections interfere constructively for certain critical angles of incidence, to cause enhanced overall reflection (also called diffraction or scattering). In acoustic diffraction, the role of the atomic planes is assumed by planes of compression and rarefaction, induced by ultrasonic waves with frequencies between 1 MHz and 2 GHz. As a result, similar diffraction effects occur as in crystals.

The similarity between atomic planes and sound wave fronts should, however, not be carried too far. For one thing, atomic planes are sharply defined in location and regular in structure. Sound waves, on the other hand, are essentially sinusoidal and, when limited in the transverse direction, spread as they propagate, thereby giving rise to very complex density distributions and wavefronts. To a first approximation however, the analogy is very useful.

The fact that the sound wavefronts move causes the diffracted light to be Doppler shifted. Brillouin predicted a basic Doppler shift equal to the sound frequency. This phenomenon of frequency shifting became of importance only in recent times and forms, in fact, the basis of heterodyning techniques in modern signal processing applications.

Long before such sophisticated techniques became practical through the invention of the laser, the application of acousto-optics as such to (parallel) signal processing had become evident, and experiments were already in progress using arc lamps and other conventional light sources. The pioneer in this field is probably Okolicsanyi who, in the early 1930's used acousto-optic techniques in the Scophony television projector [4]. In the course of this work Okolicsanyi made a thorough investigation of possible sound cell applications (for instance time compression) which he published in 1937 [5].

Manuscript received August 14, 1980.
The author is with the Department of Electrical and Computer Engineering, University of Iowa, Iowa City, IA 52242.

It was not until the early 1960's that the subject was taken up again when signal processors were investigated by Rosenthal [6], Liben [7], Slobodin [8] and Arm *et al.* [9]. By the end of the 1960's lasers were beginning to be used routinely which in turn led to the development of coherent heterodyne detection techniques by King *et al.* [10] and Whitman *et al.* [11]. Thus, almost 50 years after Brillouin's analysis, all the phenomena he predicted had been put to use.

During the past decade even more refined techniques of signal processing were developed, in particular ones involving crossed sound cells (two-dimensional processing) and time integration. A detailed discussion of this development is outside the scope of this introduction. The interested reader will find abundant information in a number of review articles [12]-[17], as well as in subsequent papers in this issue.

In what follows, the author will first give a brief, heuristic explanation of acousto-optic effects, emphasizing the plane wave interaction model but tracing, wherever practical, the connection with other, perhaps more familiar models. Next, some configurations that form the building blocks of most signal processors will be reviewed. This paper will be limited to the basic elements and avoid system details such as lens configurations, dynamic range considerations, intermodulation effects, etc. A discussion of such details is not appropriate for this brief review; they can best be learned from the papers that follow.

II. Heuristic Theory

As pointed out in the Introduction, Brillouin's analysis of acousto-optic interactions predicted an effect, now called acoustic Bragg diffraction, similar to X-ray diffraction in crystals. The principle of acoustic Bragg diffraction is illustrated in Fig. 1 which shows a beam of light directed at a high frequency sound wave. At certain critical angles of incidence $\pm\alpha_B$, the incident beam generates a new one whose direction differs by $2\alpha_B$. The angle α_B is called the Bragg angle and is given by

$$\sin \alpha_B = \frac{\lambda}{2\Lambda} \tag{1}$$

where λ is the wavelength of light in the acoustic medium and Λ is the acoustic wavelength.

The value given by (1) refers to the angle observed inside the medium of sound propagation. Outside the medium, Snell's law changes the value of α_B to α_B'

$$\sin \alpha_B' = \frac{n\lambda}{\Lambda} = \frac{\lambda_v}{\Lambda} \tag{2}$$

0018-9219/81/0100-0048$00.75

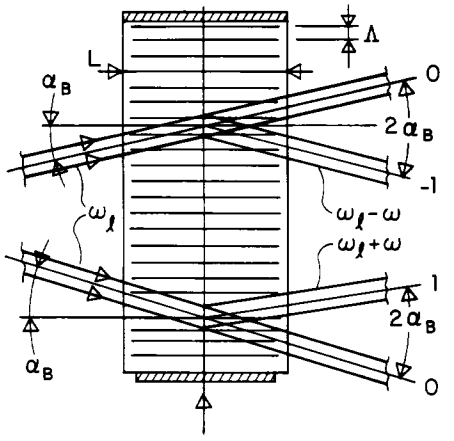

Fig. 1. Diffraction in the Bragg region showing downshifted (top) and upshifted (bottom) interaction.

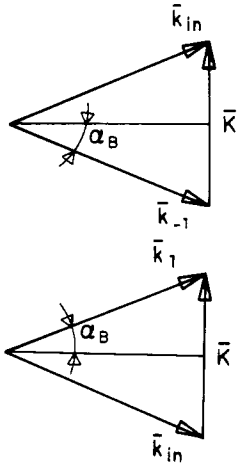

Fig. 2. Wave vector diagrams illustrating diffraction in the Bragg region for downshifted (top) and upshifted (bottom) interaction.

where λ_v denotes the vacuum wavelength. In the drawings, this refraction effect is not shown; for simplicity beams are shown propagating in the direction appropriate to the medium.

If the wavefronts of the sound move away from the incident light (Fig. 1, top), they also move away from the diffracted beam which is called the -1 order in this case. It is easily shown that this results in a negative Doppler shift, i.e., the diffracted light is downshifted in frequency by the sound frequency ω. The case of upshifted Bragg diffraction is also shown in Fig. 1 (bottom); the diffracted light is now called the +1 order.

The essential properties of Bragg diffraction can be explained in many different ways [18]-[22]. This author's preference lies with the model in which the interaction is thought of as a collision between photons and phonons. The momenta of the interacting particles are given by $\hbar\bar{k}$ and $\hbar\bar{K}$ for the photons and phonons respectively, where $\hbar = h/2\pi$, h is Planck's constant, $\bar{k}$ and $\bar{K}$ are the propagation vectors of light and sound. Conservation of momentum is then illustrated by the diagrams of Fig. 2, from which the Bragg angle conditions can be derived easily [18]

$$\sin \alpha_B = \tfrac{1}{2} K/k = \tfrac{1}{2} \lambda/\Lambda. \tag{3}$$

Frequency up- or downshift follow from the same diagrams by considering energy conservation in terms of photon—and phonon energies $\hbar\omega_l$ and $\hbar\omega$.

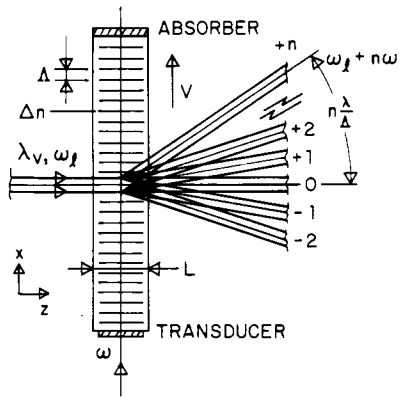

Fig. 3. Diffraction in the Debye-Sears region showing many generated orders.

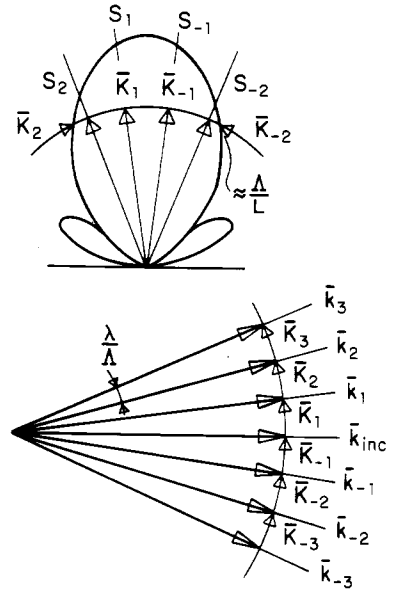

Fig. 4. Multiple scattering in the Debye-Sears region (bottom) made possible by the presence of many plane waves of sound in the radiation pattern of the transducer (top).

Note that, classically, the diagrams of Fig. 2 represent phase synchronous interaction, a concept which was already implicit in Brillouin's early paper.

If the width of the transducer L is decreased, as in Fig. 3, the column of sound in the medium will look less and less like a plane wave. More accurately, the angular plane wave spectrum of the soundfield (i.e., the radiation pattern) broadens so as to make available additional plane waves of sound for a wider range of interaction. The basic idea is shown in Fig. 4. The first effect of shortening L is that the up-and-down-shifted orders $\bar{k}_1$ and $\bar{k}_{-1}$ are now both generated due to the simultaneous presence of soundwaves $\bar{K}_1$ and $\bar{K}_{-1}$ with amplitudes S_1 and S_{-1}. If L is decreased further, additional soundwaves $\bar{K}_2$ and $\bar{K}_{-2}$ appear, with amplitudes S_2 and S_{-2}, which interact with already scattered lightwaves $\bar{k}_1$ and $\bar{k}_{-1}$ to generate the second orders $\bar{k}_2$ and $\bar{k}_{-2}$. If we continue to decrease L, more and more orders are generated, as shown in Fig. 3. (Note that the nth order is shifted in frequency by an amount $n\omega$.) The extent to which this multiple scattering process can operate is determined by the ratio of the angular width Λ/L, of the sound radiation pattern to the separation λ/Λ between orders. Customarily a parameter Q, inversely proportional

to this ratio, is used [23]

$$Q = \frac{K^2 L}{k} = 2\pi \frac{\lambda L}{\Lambda^2} . \tag{4}$$

Thus the condition for Bragg diffraction (the Bragg region) is stated as

$$Q \gg 1 \tag{5}$$

while the opposite condition denotes the multiple scattering regime where many orders may be generated. This latter regime is called the Raman-Nath [24], Lucas-Biquard, or Debye-Sears region after early investigators.

Conventionally, Debye-Sears diffraction is analyzed by using a moving phase grating model as was first done by Raman and Nath [24]. This approach can be shown to lead to the same results as are obtained by using multiple scattering calculations [25], [26]. The amplitude of the diffracted orders is given by

$$A_n = (-j)^n E_{\text{inc}} J_n(kC|S|L/2). \tag{6}$$

where E_{inc} is the amplitude of the incident light, $|S|$ represents the peak condensation or strain in the soundfield $S(x, t) = |S| \cos(\omega t - kx)$, and C is a material constant in terms of which the refractive index variation is given by

$$\Delta n(x, t) = \tfrac{1}{2} nCS(x, t). \tag{7}$$

With (7) it is easily shown that (6) may also be written as

$$A_n = (-j)^n E_{\text{inc}} J_n(\hat{\alpha}) \tag{8}$$

where $\hat{\alpha} = k_v \hat{\Delta} nL$ denotes the peak phase shift of the light due to the peak refractive index variation $\hat{\Delta} n$, and $k_v = 2\pi/\lambda_v$.

The constant C is related to the so called strain-optic coefficient p by

$$C = -n^2 p. \tag{9}$$

More generally [18], n is a tensor and strictly speaking, equation (9) applies only to liquids.

Fig. 5 shows the dependence of the diffracted orders on $\hat{\alpha}$, leaving out the $(-j)^n$ form. Quite often a modest sound pressure is used (weak interaction, $\hat{\alpha} \ll 1$) and effectively only the +1 and -1 orders are generated. In that case (6) may be approximated by

$$A_o = E_{\text{inc}}$$
$$A_{\pm 1} = -jE_{\text{inc}} \cdot \tfrac{1}{4} kC|S|L. \tag{10}$$

The situation in the Bragg region may be analyzed by using a model of two coupled modes, i.e., E_o and E_1 (or E_{-1}), as was first done by Van Cittert [27]. The results are given by

$$E_o = E_{\text{inc}} \cos(kC|S|L/4) = E_{\text{inc}} \cos\left(\frac{\hat{\alpha}}{2}\right)$$
$$E_{\pm 1} = -jE_{\text{inc}} \sin(kC|S|L/4) = -jE_{\text{inc}} \sin\left(\frac{\hat{\alpha}}{2}\right). \tag{11}$$

This behavior is illustrated in Fig. 6. For weak interaction ($\hat{\alpha} \ll 1$), the expressions (11) become identical to (10), with the understanding though, that only one order is effectively generated.

For maximum efficiency in Bragg diffraction it is necessary that $\hat{\alpha} = \pi$. It is easily shown that the required acoustic intensity is given by

$$I_s = \lambda_v^2 / 2M_2 L^2 \tag{12}$$

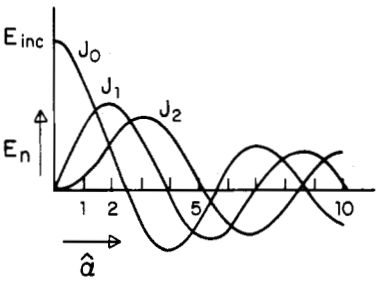

Fig. 5. Amplitude of diffracted orders versus peak phase shift $\hat{\alpha}$ in the Debye-Sears region.

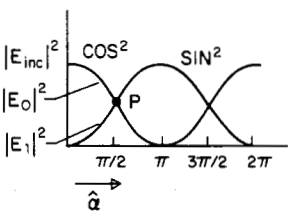

Fig. 6. Intensity of diffracted orders versus peak phase shift $\hat{\alpha}$ in the Bragg region.

where M_2 is a figure of merit [18], [28] defined by the material properties of the acoustic medium

$$M_2 = n^6 p^2 / \rho V^3 . \tag{13}$$

In (13), ρ represents the density of the medium and V the sound velocity. In practice, diffraction efficiencies range from $\simeq$95 percent at 100 MHz to $\simeq$10 percent at 2000 MHz.

III. Applications

It will be clear immediately that a sound cell may be used to modulate light, either in the Raman-Nath mode or the Bragg mode. The latter is illustrated in Fig. 7 where the sinusoidal contour of the sound beam represents amplitude modulation of the carrier. It is readily recognized that the maximum modulation frequency f_m is reached when the modulation wavelength Λ_m equals the diameter d of the light beam

$$f_{m\,(\max)} = \frac{V}{d} = \frac{1}{\tau} . \tag{14}$$

At this frequency, the effective modulation drops to zero. In (14), the parameter τ signifies the transit time of the sound through the light beam. To achieve a high f_m, the light beam is often focused into the cell, thus decreasing d and τ.

For a linear modulation transfer, the Bragg cell must be operated near a linear region of the light intensity versus sound/pressure curve, such as illustrated by point P in Fig. 6. Operation near the origin results in a linear relation between light amplitude and sound pressure.

Another application of Bragg diffraction is beam deflection. This is illustrated in Fig. 8, where the diffracted beam of light is shown in three successive positions, corresponding to sound frequencies f_1, f_2, and f_3. Because the relation between deflection angle and frequency sweep is linear,

$$\alpha_{\text{defl}} = \frac{\lambda}{V} f \tag{15}$$

a simple frequency sweep is all that is needed to operate a beam deflector. In such a device the number of resolvable angles N is determined by the ratio of the range of deflection

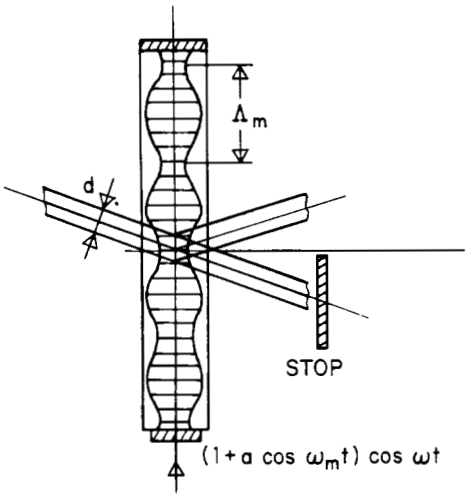

Fig. 7. Bragg diffraction sound cell used as modulator.

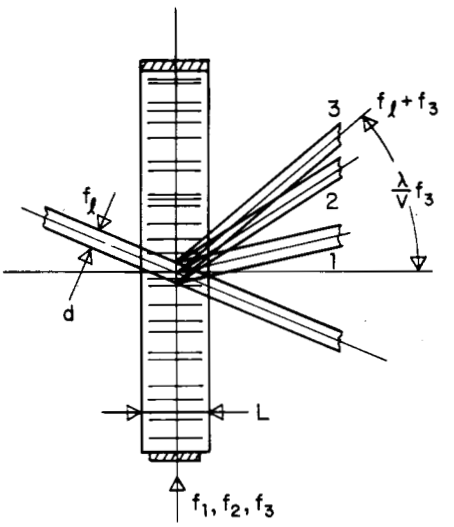

Fig. 8. Bragg diffraction sound cell used as beam deflector.

angles $\Delta\alpha_{defl}$ to the angular spread λ/d of the light beam

$$N = \frac{\Delta\alpha_{defl}}{\lambda/d} \tag{16}$$

As $\Delta\alpha_{defl}$ is determined by the maximum frequency deviation Δf through (15)

$$\Delta\alpha_{defl} = \frac{\lambda}{V}\Delta f \tag{17}$$

we may combine (16) and (17) to find

$$N = \frac{d}{V}\Delta f = \tau\Delta f. \tag{18}$$

Note that, if the deflector is used to randomly access N positions by using N different frequencies within Δf, τ also connotes the access time of the system. Likewise, for general signal processing, the parameter $\tau\Delta f$ represents the cell's time–bandwidth product. Considerations of maximum optical aperture and finite acoustic loss limit this product at present to values of 1000–2000, with τ ranging from 1 μs to 10 μs and Δf from 10 MHz to 1 GHz.

The extent to which a beam deflector works satisfactorily over its entire range depends on whether a wide enough spectrum of plane waves is available in the radiation pattern of the transducer to satisfy the Bragg angle condition at all frequencies. The condition for this is given by

$$\frac{\Lambda_{nom}}{L} > \frac{1}{2}\frac{\lambda}{V}\Delta f$$

or

$$L < \frac{2\Lambda^2_{nom}}{\lambda}\cdot\frac{f_{nom}}{\Delta f} \tag{19}$$

where Λ_{nom} and f_{nom} are the nominal sound wavelength and frequency respectively. Equation (19) indicates that for large Δf the interaction length L must be decreased. This, however, reduces the overall efficiency (see (12)), and also increases the strength of additional orders by moving out of the Bragg region (see (5)). Such difficulties may be circumvented by using a phased array transducer, designed in such a way that the frequency-dependent change in sound beam direction tracks the Bragg angle [29].

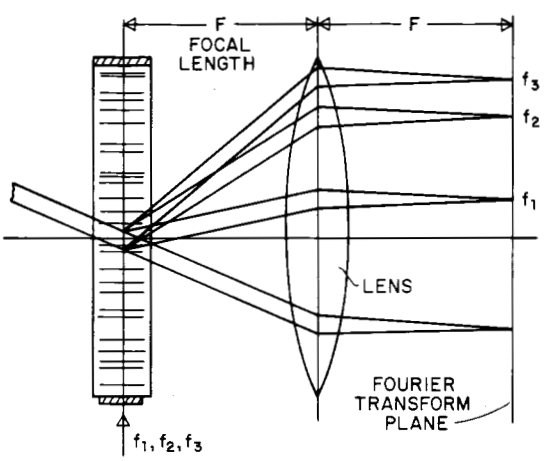

Fig. 9. Bragg diffraction sound cell used as spectrum analyzer.

One other aspect of the beam deflectors is of importance; it has to do with the rate of change df/dt of the instantaneous frequency in the soundcell. If this is large, a considerable frequency gradient (and hence deflection angle gradient) can appear across the light beam. At first glance it may be thought that this would impair the optical performance. It may be shown, however, that, for a linear frequency sweep, the effect is merely that of an additional positive or negative cylinder lens which moves up with the sound beam [30]. The focal length F of the lens is given by [18]

$$F = \frac{V^2}{\lambda}\left(\frac{df}{dt}\right)^{-1}. \tag{20}$$

If, in Fig. 8, the frequencies f_1, f_2, f_3 are fed into the sound cell simultaneously rather than sequentially, the device acts as a spectrum analyzer. Each frequency generates a beam at a specific angle; if desired, a subsequent lens will focus these beams in its back focal plane as shown in Fig. 9. This plane will then display the frequency spectrum or Fourier transform of the sound signal. It is important to realize that this is indeed a "true" frequency spectrum and not just a display of brightness versus frequency. This comes about because each beam is actually shifted in frequency by the spectrum component that generated it; also, both its amplitude and phase

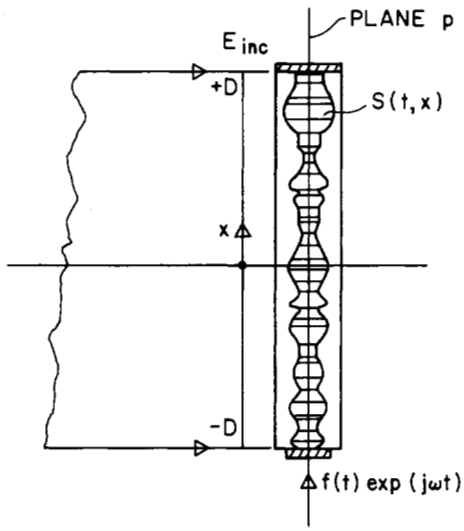

Fig. 10. Typical input configuration of an acousto-optic signal processing system.

are directly related to that component. Having available this "physical" Fourier transform makes it possible to perform complex filtering operations by optical heterodyning [11].

The spatial resolution in the Fourier transform plane corresponds to a frequency resolution $\delta f = 1/\tau$ as is to be expected from processing time considerations. Of late, efforts have been made to increase this limiting resolution by further electronic processing in the frequency plane [15]-[17]. One of the ways to achieve this is by means of an array of photodiodes subject to an optical local oscillator field of which the local frequency varies from diode to diode. Coincidence of local oscillator frequency and signal frequency at a particular diode location leads to a dc component in the heterodyne current through that diode, thereby causing an additional charge on its capacitance. The total charging time before sampling determines the signal averaging and hence the frequency resolution.

Quite frequently, signal processing is performed in an image plane of the soundcell, rather than in a Fourier transform plane. In such cases the signal processing operations are expressed by convolutions and correlations of a signal with reference fields or reference masks in an image plane [13], [14], rather than direct or conjugate multiplications through optical heterodyning or masking in the Fourier transform plane. Both techniques are of course equivalent [12]; the choice is mainly a matter of convenience.

A typical input system for image plane processing is shown in Fig. 10. The signal fed to the transducer is assumed to be modulated in both phase and amplitude, hence of the general form

$$\text{Re}\,\{f(t)\exp(j\omega t)\} \tag{21}$$

where, for amplitude modulation, $f(t) = A(1 + a\cos\omega_m t)$ and, for phase modulation $f(t) = A\exp[j\phi(t)]$. The constant A is, in general, complex. If the origin of the coordinate system is located in the center of the cell, the sound field may be written:

$$S(t,x) = \text{Re}\left[s\left\{t - \frac{(x+D)}{V}\right\}\exp j\{\omega t - K(x+D)\}\right] \tag{22}$$

where $2D$ is the length of the sound cell and $s(t,-D) \propto f(t)$.

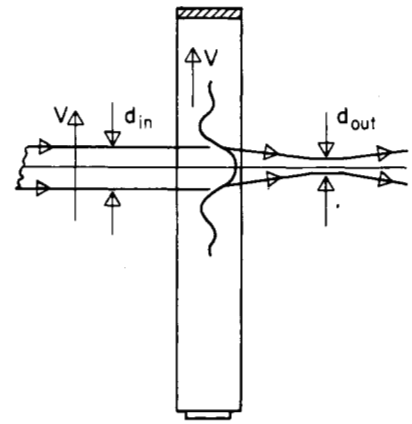

Fig. 11. Acousto-optic traveling lens, showing spot demagnification for increase of resolution.

Fig. 10 shows the light perpendicularly incident on the sound cell, as is appropriate for Raman-Nath interaction. Let E_{inc} be the amplitude of the incident light, referred to plane p through the center of the cell. For weak interaction, the exit light, also referred to plane p, may then be approximately written [12] (in complex notation)

$$\begin{aligned} E_{\text{exit}} \simeq E_{\text{inc}} &+ \\ &-\frac{1}{4}jkCL\cdot E_{\text{inc}}\, s\left\{t - \frac{(x+D)}{V}\right\} \\ &\cdot\exp\{j(\omega_c+\omega)t - jK(x+D)\} \\ &-\frac{1}{4}jkCL\cdot E_{\text{inc}}\, s^*\left\{t - \frac{(x+D)}{V}\right\} \\ &\cdot\exp\{j(\omega_c-\omega) + jK(x+D)\} \end{aligned} \tag{23}$$

where the asterisk denotes the complex conjugate. The second term in (23) gives rise to the plus first-order scattered light, the third term to the minus first order. This is most easily seen by taking s to be constant: the second term then describes the cross section of a light beam propagating in the direction $\alpha_{+1} \simeq K/k$, the third term refers to a beam in the direction $\alpha_{-1} \simeq -K/k$.

Note that the downshifted field is described by s^* rather than s; as either of the two fields may be used for further processing (the other one and the zeroth-order field can be removed by suitable stops in a focal plane), it is easily conjectured that both correlation (needing a conjugate term) and convolution may be achieved with suitable configurations.

For Fig. 10 to describe a Bragg diffraction configuration, the light must be incident at the appropriate Bragg angle. The exit light is then still described by (23) with the understanding that either the second or the third term be absent. Due to the frequent need for systems with large bandwidth and hence high carrier frequency, Bragg diffraction signal processing is more common (see (5)).

Early descriptions of acousto-optic signal processing often model the action of the sound cell, in qualitative terms, as carrying a moving replica of the electrical signal [5]. Modern accounts usually talk about parallel processing.

All of the applications described so far rely on diffraction effects. This requires that many wavelengths of sound are simultaneously present within the lightbeam. Where this condition is not satisfied, any possible effects are better analyzed on the basis of ray bending. Such refractive effects are often

useful in their own right. An example of some importance to various signal processing schemes is the so called traveling lens [31]. Fig. 11 shows the principle of operation. A high level pulse of sound is launched into an acoustic medium and the central part of it used to focus an incoming light beam of diameter d_{in} into a smaller diameter d_{out}. It is necessary that the incoming beam track the sound pulse, but that may conveniently be achieved by an acousto-optic beam deflector. Traveling lenses have been successfully operated to extend the resolution of beam deflectors by factors of 10 or more [32].

Many more details and applications of acousto-optics could be discussed such as polarization effects, birefringence, Bragg diffraction imaging, guided wave effects, etc. This short review has necessarily been limited to some fundamental aspects of immediate concern to signal processing. The interested reader will find excellent discussions of subjects neglected here, in the review articles cited in the text.

References

[1] L. Brillouin, "Diffusion de la lumière et des rayons X par un corps transparent homogène," *Ann. Phys. (Paris)*, vol. 17, pp. 88–122, 1922.

[2] R. Lucas and P. Biquard, "Propriétés optiques des milieux solides et liquides soumis aux vibration élastiques ultra sonores," *J. Phys. Rad.*, vol. 3, pp. 464–477, 1932.

[3] P. Debye and F. W. Sears, "On the scattering of light by supersonic waves," *Proc. Nat. Acad. Sci.* (U.S.), vol. 18, pp. 409–414, June 1932.

[4] D. M. Robinson, "The supersonic light control and its application to television with special reference to the Scophony television receiver," *Proc. IRE*, vol. 27, pp. 483–486, Aug. 1939.

[5] F. Okolicsanyi, "The wave-slot, an optical television system," *Wireless Engineer*, vol. 14, pp. 527–536, Oct. 1937.

[6] A. H. Rosenthal, "Application of ultrasonic light modulation to signal recording, display, analysis and communication," *IRE Trans. Ultrason. Eng.*, vol. UE-8, pp. 1–5, Jan. 1961.

[7] W. Liben, "Some applications of an ultrasonic light modulator," *J. Acoust. Soc. Amer.*, vol. 34, pp. 860–861, June 1962.

[8] L. Slobodin, "Optical correlation technique," *Proc. IEEE*, vol. 51, p. 1782, Dec. 1963.

[9] M. Arm, L. Lambert, and I. Weissman, "Optical correlation technique for radar pulse compression," *Proc. IEEE*, vol. 52, p. 842, July 1964.

[10] M. King, W. R. Bennett, L. B. Lambert, and M. Arm, "Real time electro-optical signal processors with coherent detection," *Appl. Opt.*, vol. 6, pp. 1367–1375, Aug. 1967.

[11] R. Whitman, A. Korpel, and S. Lotsoff, "Application of acoustic Bragg diffraction to optical processing techniques," in *Proc. Symp. Modern Optics*, pp. 243–255, 1967.

[12] A. Korpel, "Acousto-optic signal processing," in *Optical Information Processing*, Yu E. Nesterikhin and G. W. Stoke, Eds. New York: Plenum, 1976, ch. 10, pp. 171–194.

[13] R. A. Sprague, "A review of acousto-optic signal correlators," *Opt. Eng.*, vol. 16, pp. 467–474, Sept./Oct. 1977.

[14] L. N. Flores and D. L. Hecht, "Acousto-optic signal processors," in *SPIE Conf. Proc.*, vol. 118, pp. 182–192, 1977.

[15] P. Kellman, "Time integrating optical processors," in *SPIE Conf. Proc.*, vol. 185, pp. 130–139, 1978.

[16] T. M. Turpin, "Time integrating optical processors," in *SPIE Conf. Proc.*, vol. 154, pp. 196–203, 1978.

[17] T. R. Bader, "Acousto-optics spectrum analysis," *Appl. Opt.*, vol. 18, pp. 1668–1672, June 1979.

[18] A. Korpel, "Acousto-optics," in *Applied Solid State Science, Vol. 3*, R. Wolfe, Ed. New York: Academic Press, 1972, ch. 2, pp. 73–179.

[19] ——, "Acousto-optics," in *Applied Optics and Optical Engineering*, Vol. VI, R. Kingslake and B. J. Thompson, Eds. New York: Academic Press, 1980, ch. 4, pp. 89–136.

[20] R. Adler, "Interaction between light and sound," *IEEE Spectrum*, vol. 4, pp. 42–53, May 1967.

[21] E. I. Gordon, "A review of acousto-optical deflection and modulation devices," *Proc. IEEE*, vol. 54, pp. 1391–1401, Oct. 1966.

[22] C. F. Quate, C. D. W. Wilkinson, and D. K. Winslow, "Interaction of light and microwave sound," *Proc. IEEE*, vol. 53, pp. 1604–1622, Oct. 1965.

[23] W. R. Klein and B. D. Cook, "Unified approach to ultrasonic light diffraction," *IEEE Trans. Sonics Ultrason.*, vol. SU-14, pp. 723–733, July 1967.

[24] C. V. Raman and N. S. Nagendra Nath, "The diffraction of light by high frequency sound waves," *Proc. Ind. Acad. Sci.*, vol. 2, pp. 406–420, 1935; vol. 3, pp. 75–84, 1936; vol. 3, pp. 119–125, 1936; vol. 3, pp. 459–465, 1936.

[25] A. Korpel, "Two-dimensional plane wave theory of strong acousto-optic interaction in isotropic media," *J. Opt. Soc. Amer.*, vol. 69, pp. 678–683, May 1979.

[26] A. Korpel and T. C. Poon, "An explicit formalism for acousto-optic multiple plane wave scattering," *J. Opt. Soc. Amer.*, vol. 70, pp. 817–820, July 1980.

[27] P. H. Van Cittert, "Zur Theorie der Lichtbeugung an Ultraschallwellen," *Physica IV*, pp. 590–594, July 1937.

[28] T. M. Smith and A. Korpel, "Measurement of light-sound interaction efficiencies in solids," *IEEE J. Quantum Electron.*, vol. QE-1, pp. 283–284, Sept. 1965.

[29] A. Korpel, R. Adler, P. Desmares, and W. Watson, "A television display using acoustic deflection and modulation of coherent light," *Appl. Opt.*, vol. 5, pp. 1667–1675, Oct. 1966; *Proc. IEEE*, vol. 54, pp. 1429–1437, Oct. 1960.

[30] J. S. Gerig and H. Montague, "A simple optical filter for chirp radar," *Proc. IEEE*, vol. 52, p. 1753, Dec. 1964.

[31] L. C. Foster, C. B. Crumley, and R. L. Cohoon, "A high resolution optical scanner using a traveling wave acoustic lens," *Appl. Opt.*, vol. 9, p. 2154, 1970.

[32] S. K. Yao, D. Weid, and R. M. Montgomery, "Guided acoustic wave traveling lens for high speed optical scanners," *Appl. Opt.*, vol. 18, pp. 446–453, Feb. 15, 1979.